Journal of Ceramic Processing Research. Vol. 1, No. 1, pp. 45~52 (2000)

J O U R N A L O F
Ceramic
Processing Research

The mechanism of gold deposition by thermal evaporation

Mark C. Barnes, Doh-Y. Kim and Nong M. Hwang[a,*]
[a]Center for Microstructure Science of Materials, Seoul National University, Seoul 151-742, Korea
Korea Research Institute of Standards and Science, PO Box 102, Daejon 305-600, Korea

The charged cluster model states that chemical vapor deposition (CVD) begins with gas phase nucleation of charged clusters followed by cluster deposition on a substrate surface to form a thin film. A two-chambered system, separated by a 1-mm orifice, was used to study gold deposition by thermal evaporation in order to determine if the CCM applies in this case. At a filament temperature of 1523 and 1773 K, the presence of nano-meter sized gold clusters was confirmed by transmission electron microscopy (TEM). The charge on the primary clusters was found to be positive and the cluster size and size distribution increased with increasing temperature. Small clusters were found to be amorphous and they combined with clusters already deposited on a substrate surface to form larger amorphous clusters on the surface. This work revealed that gold thin films deposited on a mica surface are the result of the sticking of 4~10 nm clusters. The topography of these films was similar to those reported previously under similar conditions.

Key words: Gold, Evaporation, Thin film, Clusters, Deposition.

Introduction

A recently proposed model for chemical vapor deposition (CVD), the charged cluster model (CCM), is based on CVD being initiated by gas phase nucleation of charged clusters and subsequent cluster deposition on a substrate surface [1-7]. The concept of the CCM is similar to the ionized cluster beam deposition (ICBD) method [8]. However in the CCM, charged or ionized clusters are formed in the gas phase of the thin film reactor without intentional efforts of making clusters such as adiabatic nozzle expansion.

Nanometer sized charged clusters have been shown to make perfect films by thermal motion without the highly energetic impact that is used in ICBD by applying electric field in a high vacuum chamber of long mean-free-path. There are two reasons why such clusters have gone unnoticed during thin film deposition. One is that the clusters are difficult to detect without a specially designed technique due to their nanometer size. The other is that these clusters can make a perfect film that is indistinguishable from a film deposited by the atomic unit. The ability of clusters to produce a dense film may be explained by Fujitas concept of magic size [9], below which the clusters have liquid-like properties in deformation and diffusion. The marked melting point depression of nanometer clusters [10, 11] might also be related to this phenomenon.

*Corresponding author:
Tel: +82-2-880-8922
Fax: +82-2-882-8164
e-mail: nmhwang@kriss.re.kr

Adachi *et al.* [12-15] and Okuyama *et al.* [16] not only confirmed the existence of the gas phase nucleated particles in a non-plasma CVD reactor but also suggested that the particles contributed to film deposition. Previously, it was generally believed that particles generated during the CVD process did not contribute to film deposition and the incorporation of the particles into the film was believed to significantly impair the film quality [17].

Charge plays the most important role in maintaining the nanometer size of clusters by providing Coulombic repulsion between charged clusters. Neutral clusters undergo Brownian coagulation and form macro particles relatively easily, eventually leading to a porous skeletal film. In the plasma or hot filament CVD process, the presence of charge in abundance is evident. In thermal CVD and evaporation processes, the presence of charge in an appreciable amount is not expected. However, in measuring the electric current in the reactor, an appreciable amount of charge is almost always accompanied in the condition of film deposition.

Once gas phase nucleation occurs in the thin film process, the total surface area of a nanosized particle is so large that most of the supersaturation for precipitation disappears, reducing the driving force for deposition markedly. Normally, the remaining supersaturation comes from the capillary effect of the nanosized particles. In some cases of CVD, the solubility of a solute in the gas phase is retrograde or increases with decreasing temperature, in which case gas phase nucleation causes an etching driving force at the substrate. In this case, etching by the atomic or molecular unit and deposition by the nanosized particles takes place

simultaneously. If this phenomenon is observed macroscopically, it appears that two irreversible processes of deposition and etching take place simultaneously in opposite directions under the same thermodynamic condition. This is against the second law of thermodynamics if the deposition unit is atom or molecule because the driving force can be either for deposition or for etching but cannot be for both.

Therefore, observation of simultaneous deposition and etching in the system with the retrograde solubility provides evidence that the films were deposited exclusively from the nanometer-sized particles with the atomic flux contributing negatively to film formation. C-H and Si-Cl-H systems have the retrograde solubility in the temperature range of interest. The C-H system can be used to synthesize diamond if a hot filament or plasma process is used. In this case, it is well established that the less stable diamond deposits and simultaneously stable graphite etches under the same conditions [1]. In the Si-Cl-H system, Si deposits and etches simultaneously under the same conditions. The selective epitaxial growth of silicon by the CVD process has since been shown to occur by this mechanism [4]. Nanometer silicon clusters in the gas phase were experimentally confirmed during the silicon CVD process in the Si-Cl-H system [6]. The presence of nanometer diamond clusters in the gas phase has been confirmed also [7]. The deposition of ZrO_2 by the CVD process [4] and the deposition of W films by thermal evaporation [5] also took place by this mechanism. Considering this, the possibility of this mechanism applying to other thin film processes such as the thermal evaporation of gold, is being investigated in this report.

Thin films can be deposited by thermal evaporation of a metal in a tungsten basket used as a hot-filament. Mahoney *et al.* [19] investigated two methods of gold deposition and compared gold deposited by thermal evaporation and by cluster beam deposition. They reported that the two methods of deposition resulted in similar deposition behaviors. However the possibility of automatic gas phase nucleation occurring during thin film formation was not reported.

The application of the CCM to the thermal evaporation process has some practical implications. The concept can be applied to synthesizing nanometer powders. The fact that the clusters have a relatively uniform size arising from the presence of charge can be used to make the quantum dot structure. The purpose of this study is to examine the applicability of the CCM to the thin film process by the thermal evaporation of gold. For this, we will examine the production of charge during the deposition process, the confirmation of clusters and their behavior in relation to film formation. In order to compare the surface morphology produced by cluster growth with that reported for gold deposition by other researchers, film topography as a function of substrate temperature is also reported.

Experimental

A two-chamber system was used for the simultaneous observation of both a thin film and isolated clusters. The system consists of an upper and a lower chamber, which are separated by a 1-mm ϕ orifice. The lower chamber was evacuated by a rotary and diffusion pump, which resulted in differential pumping to a pressure of 0.067 Pa and 1.33 Pa in the lower and upper chamber, respectively, before the commencement of evaporation.

A 40 mm-length gold wire (0.2 mm in diameter, 99.99% purity, Electron Microscopy Services, Washington USA) was placed in a tungsten basket used as a hot filament (The Nilaco Corporation, Tokyo, Japan). The basket was then placed in the upper chamber. In the case of experiments with a time duration > 120 s and for current measurements, 100 mm-length gold wire was used instead. Two transmission electron micro-

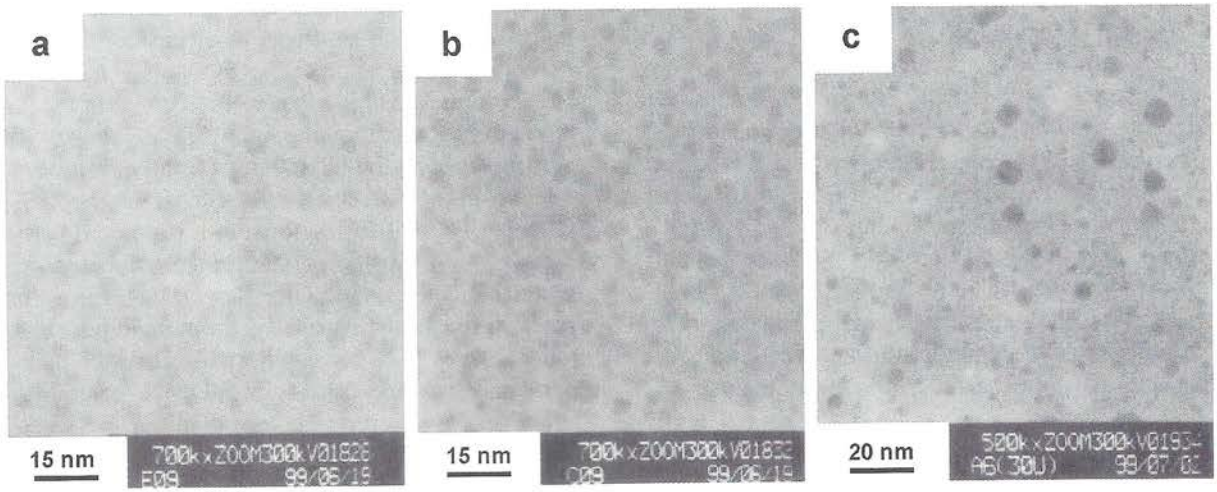

Fig. 1. Showing a comparison between TEM samples of gold deposited in the upper chamber with the exposure times of 10 (a), 15 (b) and 30 s (c).

scopy (TEM) grids (Electron Microscopy Sciences Washington USA, amorphous carbon support film on a 200 mesh Cu grid) were placed in the apparatus, one 25 mm directly below the orifice in the lower chamber and the other, 15 mm below the tungsten filament in the upper chamber. Therefore, the distance of the TEM grid in the upper and lower chamber was 15 and 40 mm below the filament, respectively. The substrate temperatures were 298 or 713 ± 20 K, measured by a thermocouple. The experimental time duration ranged from 10 to 300 s.

A constant filament temperature of 1523 or 1773 ± 25 K, determined by a thermocouple, was used in these experiments. During the experiment, the pressure increased to 6.67 Pa in the upper chamber due to gold evaporation and thermal expansion and remained largely constant throughout the experiment. For TEM sample preparation, at 1523 K, the exposure times were 15, 30, 120 and 300 s for the lower chamber and 10, 15, and 30 s for the upper chamber. In the upper chamber, a thin film began to form after 30 s, which made it difficult to observe by TEM (Hitachi, H-9000NAR). Therefore, for the time periods of 30, 120 and 300 s, Si wafer substrates were placed 15 mm below the hot-filament in the upper chamber and subsequently analyzed by scanning electron microscopy (SEM, Topcon SM-720). At 1773 K the exposure time was 30 s and instead of a TEM grid, a mica strip was placed in the lower chamber to allow for the simultaneous observation of a film and clusters. The mica strip was observed by both TEM and atomic force microscopy (AFM, Park Scientific Instruments, Autoprobe CP).

Results and Discussion

Confirmation of Charge

In order to confirm that charge is produced during the thermal evaporation of gold at 1523 K, the electric currents with and without gold in the W basket at 1523 K were compared. A bias voltage was applied from −20 to +10 volts between the electrode and the ground to determine the charge polarity. The results showed that a positive charge was produced by gold evaporation. The positive charge suggests gold ionization, and this reflects the existence of the low ionization potential of materials that are easily ionized at high temperatures. However, such appreciable atomic ionization was not expected to have occurred in this case, as the temperature was too low to overcome the atomic ionization potential of gold, which is ~9 eV [19]. This indicates that ionization after clustering occurred as clusters have an ionization potential close to the work function of the bulk metal, (~5 eV for gold) [19]. This suggests that both charged and neutral clusters may nucleate in the gas phase and this observation may apply in other metal evaporation systems. The current at −20 V was found to be ~100 nA per cm^2. If it is assumed that the current comes from charged clusters and that the cluster velocity is 100 m/s, the number density of clusters in the gas phase is estimated to be ~$10^8/cm^3$.

The observation of gold clusters up to 300 seconds at 1523 K

upper chamber Figure 1 shows a comparison between TEM samples of gold deposited in the upper chamber with the exposure times of 10, 15 and 30 s. A cluster size (2.4 ± 0.2 nm) is observed on samples after 10 and 15 s (Figs. 1(a) and (b)). No lattice fringe was observed by high resolution TEM and these clusters are thus thought to be amorphous. The number density of clusters was ~$4 \times 10^{14}/mm^2$ at 10 s and increased to ~$7.5 \times 10^{14}/mm^2$ after 15 s. In order to estimate the number of gold atoms in each cluster, a hemispherical shape approximation was assumed. It was estimated that the 2.4 ± 0.2 nm clusters contained approximately 250 ± 50 atoms. After 30 s the cluster size and size distribution increased to 12.0 ± 9 nm with none smaller than those observed in Figs. 1(a) and (b). All clusters detected on these samples (Fig. 1(c)) had no observable lattice fringe and thus concluded to be amorphous.

There are two facts that suggest that the clusters did not nucleate on the substrate but formed in the gas phase. One is the highly uniform size distribution in Figs. 1(a) and (b), which is not expected by continuous nucleation and growth on the surface. The other is the increase in number density without an appreciable increase in cluster size with time between 10 and 15 s. From this it appears that the large clusters in Fig. 1(c) did not form in the gas phase but grew by the deposition of small clusters. When clusters on the substrate continue to grow by the deposition of small clusters, they impinge each other, thereby making a film. At longer times, the presence of this film made TEM observation on TEM grids difficult. Therefore, SEM observations on Si wafers were done.

SEM photomicrographs depicting the microstructural evolution of a gold thin film from 0 to 300 s are shown in Fig. 2. After 30 s exposure in the upper chamber, the grain/particle size of the thin film is approximately 10 nm, which is consistent with TEM observations shown in Fig. 1(c). The grain size increases to approximately 20~30 nm after 120 s and between 50~100 nm after 300 s. This suggests that the film was produced by cluster deposition. In order to confirm that clusters make the thin film observed in Fig. 2, in the next section, cluster deposition in the lower chamber will be discussed.

lower chamber Figures 3(a-d) show the clusters captured on TEM grids in the lower chamber after 15, 30, 120 and 300-s deposition time, respectively. Figures 3(a) and (b) show clusters landing after a short exposure time (15 and 30 s). Figures 3(c) and (d) show

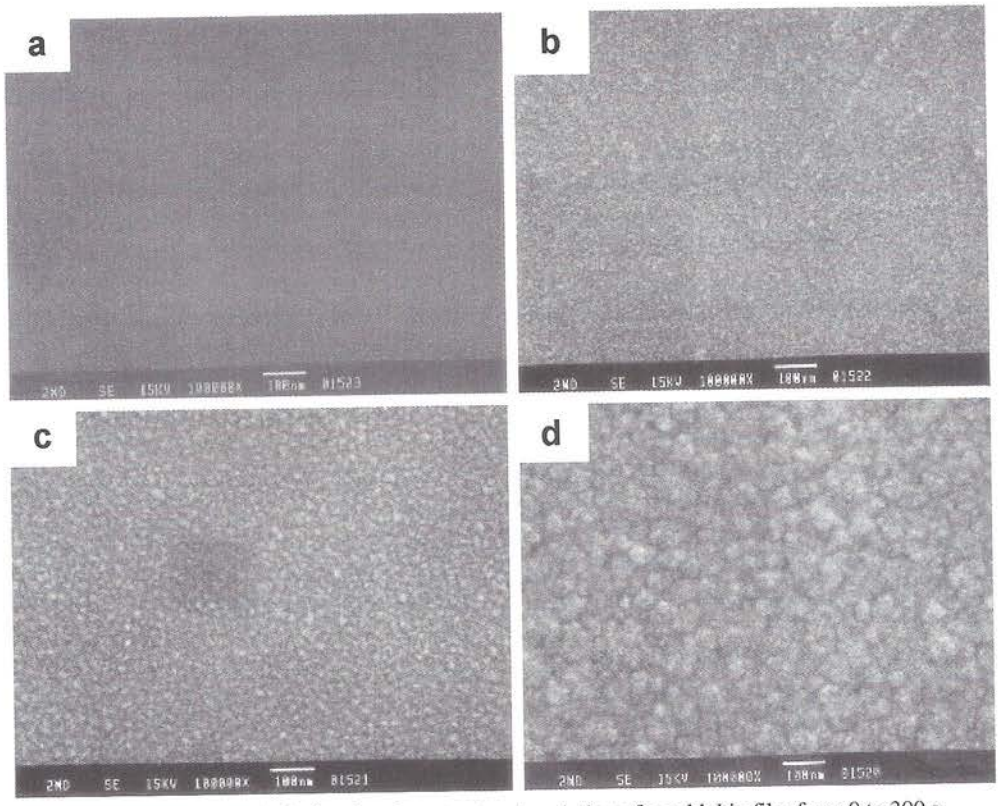

Fig. 2. Showing SEM photomicrographs depicting the microstructural evolution of a gold thin film from 0 to 300 s.

clusters landing after a long exposure time (120 and 300 s). As Figure 3 represents separate time duration areas, the discussion will be divided into short time duration (15 and 30 s) and long time duration (120 and 300 s).

In the short time duration, at both 15 and 30 s, small clusters (5.0 ± 0.3 nm) were observed with the number density on the 30 s sample ($\approx 5 \times 10^7$ mm^{-2}) being approximately twice that of the 15 s sample ($\approx 3 \times 10^7$ mm^{-2}). It can be argued that these clusters were not formed in the gas phase of the upper chamber but were formed during the adiabatic expansion of the vapor after being extracted through the orifice. If this were the case, the cluster size should be smaller than those observed in the upper chamber since the supersaturation is much higher during adiabatic expansion. However, the cluster size in the lower chamber was double that in the upper chamber.

The increase in the cluster size in the lower chamber has an important implication regarding cluster properties. The clusters may increase in size by the attachment of gold atoms during expansion but this effect cannot be so high as to explain the doubling in size. The clusters extracted into the lower chamber would undergo energetic flight of high momentum because of the pressure difference between the upper and the lower chambers. After clusters impact on the substrate with high momentum, the clusters appear to become flat. That is, the shape of clusters in the upper chamber is spherical or hemispherical but those in the lower chamber have a disc shape. Therefore, the increase in cluster radius in Figs. 3(a) and (b) compared to that in Figs. 1(a) and (b) may not come from the increase in the number of atoms but from a shape change.

If this is true, the result shows that small clusters have liquid-like properties in deformation, which was previously suggested by Fujita [9]. Besides, small clusters are known to have a lower melting temperature than the bulk material because of the high proportion of surface atoms, which are weakly bound and less constraint [20]. According to reports by Buffat *et al.* [10] and by Borel [11], the melting point depression of gold clusters that are observed in the upper chamber (2.5 nm) would be > 400 K.

Using a disc shape approximation (as they occupy a larger area), the height of the clusters in Fig. 3 was estimated to be 3.10 nm, which is approximately one gold atom in height. This is in contrast to those in the upper chamber (approximately 4 atoms for the hemispherical clusters). The cluster size did not increase over the whole 30 s period. This suggests that the cluster size in the upper chamber also did not increase. These results further reinforce the inference that the large clusters in Fig. 1(c) did not originate directly from the gas phase but grew by the addition of small clusters. In that case, Fig. 1(c) would be the initial stage of film formation by the cluster deposition.

The results of Figs. 1 and 3 confirm that clusters were formed in the upper chamber. However, it is difficult to understand the clustering process, consider-

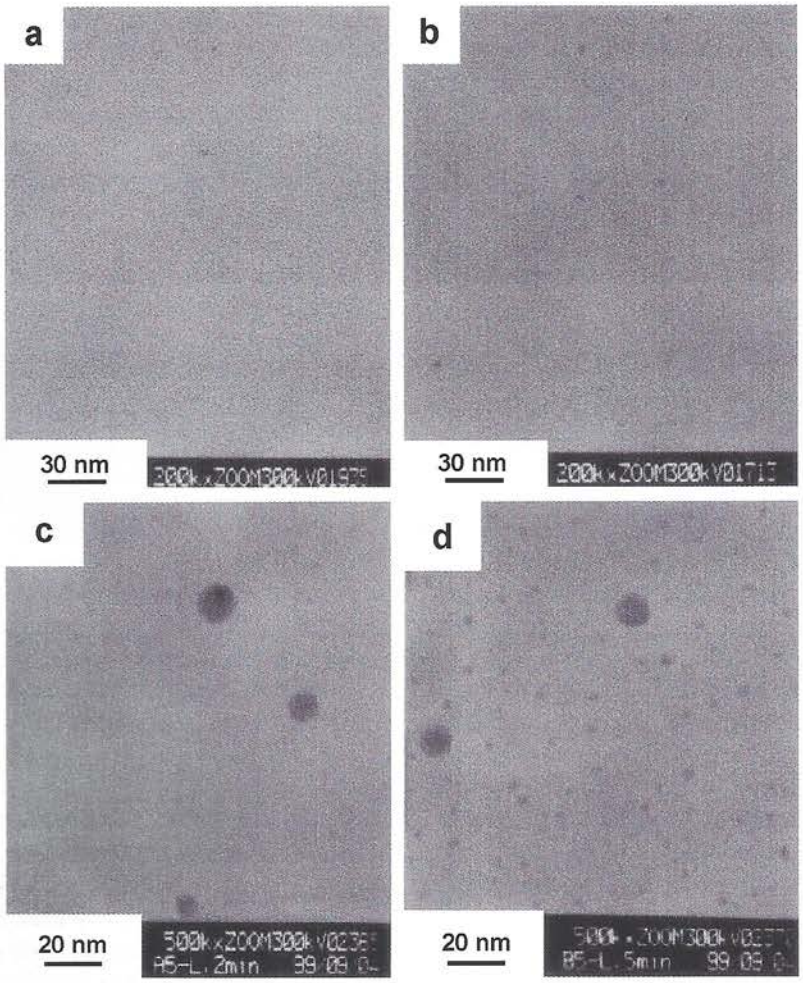

Fig. 3. Showing clusters captured on TEM grids in the lower chamber after 15, 30, 120 and 300-s deposition time, respectively. Figures 5(a) and (b) show clusters landing after 15 and 30s, respectively. Figures 5(c) and (d) show clusters landing after 120 and 300s, respectively.

ing the relatively long mean free path in the reactor during the process. The supersaturation ratios for precipitation of gold after evaporation at 1523 K are $\sim 4.9 \times 10^{18}$ and $\sim 1.1 \times 10^{10}$ at 473 K and 573 K, respectively, at the distance 1 cm away from a spherical gold source of 1 mm ϕ. Although the supersaturation ratio is very high, the mean free path is small. In an initial vacuum of 0.01 torr, the mean free path of gold atoms at 1523 K and 473 K is ~6.1 and 1.9 cm, respectively. Even after the pressure increase to 0.02 torr after filament heating to 1523 K, the mean free path at 473 K is ~1.0 cm, which is comparable to a distance of 1.5 cm between the tungsten basket and the substrate. Considering the mean free path, clustering of a few hundred gold atoms is not expected. One possibility is that there is a high temperature gradient between the filament and the orifice. A high temperature gradient would promote clustering by increasing the supersaturation with increasing distance away from the filament. In order to measure the temperature gradient, the temperature of a substrate placed in the upper chamber, insulated from the water-cooled wall, was measured and was found to be only ~323 K (measured by thermocouple). Another possibility is that the electric charge generated during evaporation may be related to clustering. A charged atom or cluster induces the image force of attraction with a neutral atom.

Figures 3(c) and (d) show clusters landing in the lower chamber after 120 s and 300 s exposure time, respectively. Here in both cases, a bimodal distribution of gold clusters can be seen. The average size of the smaller clusters after 120s exposure was 2.0 ± 0.2 nm with a number density of $\approx 9 \times 10^9$ mm^{-2}. The larger size clusters were 8.0 ± 3.0 nm in size with a number density of $\approx 6 \times 10^7$ mm^{-2}. The number of atoms/cluster was estimated to be approximately 95 ± 30 and 11000-80000 atoms, respectively. At 300 s, the size distribution and number density of the larger clusters appeared to be constant. However, the smaller clusters increased in overall size to (3.0 ± 0.2 nm), which approximates to 160 ± 40 atoms per cluster. The number density also increased to $\approx 1.4 \times 10^{10}$ mm^{-2}. The size of the smaller clusters observed at 120 and 300 s are smaller than that observed in the lower chamber at 15 and 30 s. Furthermore, in both cases the small clusters had a uniform size.

In order to explain the observation of the bimodal distribution, coulomb interactions between two spherical conductors, charged with the same sign, should be considered [8].

$$F = \frac{q_1 q_2 e^2}{4\pi\varepsilon_o d^2} - \frac{q_1^2 e^2 r_2 d}{4\pi\varepsilon_o (d^2 - r_1^2)} - \frac{q_2^2 e^2 r_1 d}{4\pi\varepsilon_o (d^2 - r_2^2)} + \cdots, \quad (1)$$

where the sphere of radius r_1 has a net charge q_1 and the other of radius r_2 has charge q_2; d is the distance between the centers and $1/4\pi\varepsilon_o$ the permittivity. In this case, small clusters would be singly charged due to the high barrier for the removal of more electrons. The equation shows that the interaction changes from repulsion to attraction as the size difference between two clusters increases. For example, if $r_2 >> r_1$ and thus $r_2 \approx >> d$, the interaction between the large and the small particles charged with the same sign can be attractive. In this case, the attraction will increase as q_2 increases. This analysis shows that the interaction between charged clusters of similar size tends to be repulsive while that between small and large ones can be less repulsive or even attractive. In the case of these experiments, the length of time (120 and 300 s) or high temperature (increased evaporation flux) can enable some clusters to grow in the gas phase. In this situation, larger clusters would grow by attachment of small ones while small clusters, which are continuously being produced, maintain their size. In the situation where there is sufficient time for growth, the presence of the bimodal size distribution seen in Fig. 3(c) and (d) and the large clusters seen in Fig. 4(b), can be explained by considering the Coulomb interaction between charged clusters, the length of time that the clusters spend in the gas phase and the evaporation flux.

TEM and AFM Observations of Deposition at 1773 K

In order to analyze further whether large clusters can form in the gas phase, the effect of increasing evaporation flux i.e. increasing the filament temperature was investigated. For comparison, Fig. 4 show clusters deposited in the lower chamber for 30 s at 1523 and 1773 K, respectively. This experiment was conducted for only 30 s as it was found that at 1773 K at 0 torr, after approximately 60 s, all the gold had evaporated. Figure 6a shows the uniformed sized clusters, 4.3 ± 0.3 nm seen in Figure 3(b), that were deposited at a filament temperature 1523 K. Increasing the temperature to 1773 K (Fig. 6(b)) resulted in an increased number of clusters (3.4×10^{10} mm^{-2}), size and size distribution (6.0 ± 4.0 nm). It should be noted that in a high flux environment, the potential for gas phase nucleation is much higher due to a lower the mean free path and higher temperature gradient. With this higher flux and lower mean free path, there is a higher potential for cluster formation and growth in the gas phase. This means that larger clusters with a larger size distribution would be expected, which is exactly what is observed. A similar result with diamond cluster formation was reported where in a high flux environment, the size distribution and mean size was much larger than in a low flux environment. In their experiments, altering the carbon concentration changed the flux [7]. In this section, modifying the filament temperature alters the flux.

Surface Topography of Thin Films This report also aimed to confirm whether gold clusters could produce a thin film. The report thus far has shown that when using a two-chambered CVD apparatus at 1523 K, only clusters in the lower chamber were captured on a TEM grid with no significant growth by the atomic unit being observed. In this section, by increasing the evaporation flux (i.e. increasing the filament temperature to 1773 K), thereby increasing the production rate of clusters, a thin film can be produced in the lower

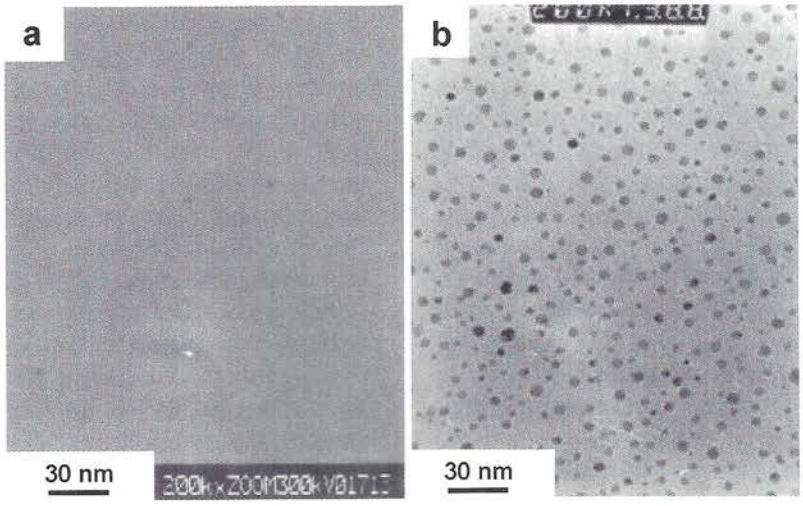

Fig. 4. Showing clusters deposited in the lower chamber for 30 s at 1523 (a) and 1773 K (b), respectively.

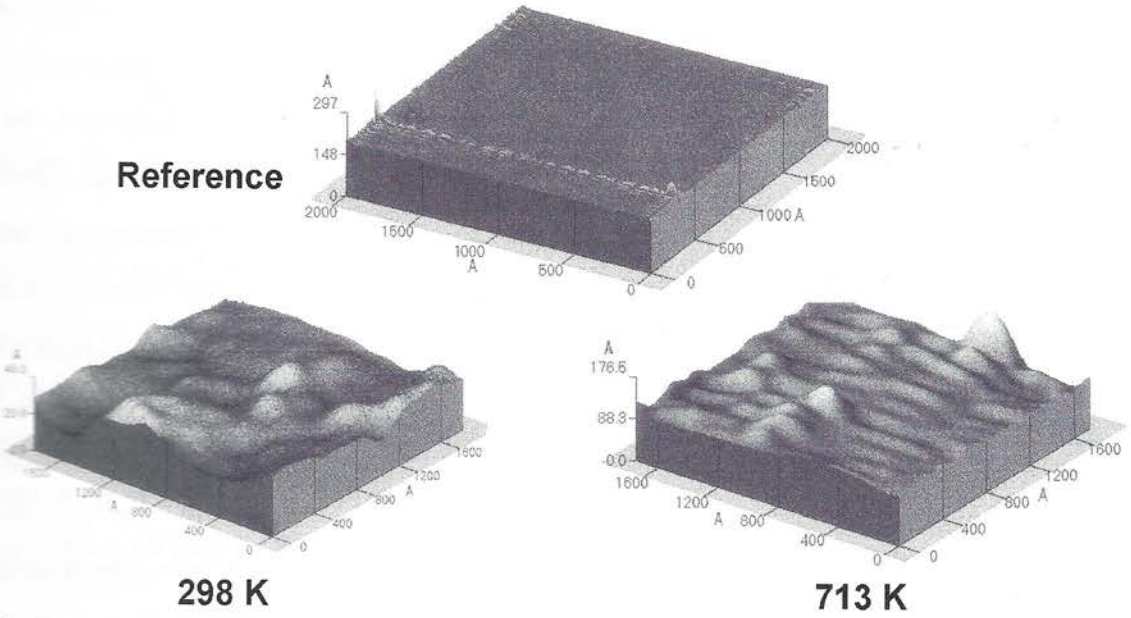

Fig. 5. Showing typical topographies of thin films deposited on mica in the lower chamber at room temperature and 713 ± 20 K compared to a reference mica strip. At 298 K, the film indeed has a rolling hill morphology similar to that produced in other studies. At 713 K the topography had changed to a hilly topography with long channels.

chamber. However, as a 1-mm f orifice separates the two chambers, there will be more deposition directly under the orifice than further away. Figure 4(b) shows deposition in the periphery of deposition. In the center, a film was observed. As clusters were confirmed in the lower chamber, it can be concluded that these clusters make up the film. Having identified that clusters produce a thin film in the lower chamber, it may be argued that the film produced by clusters is somehow different from that produced in single chamber experiments.

Therefore it is necessary to show that the thin film produced in the lower chamber at the center of deposition, by clusters is the same as reported by other researchers. Liu *et al.* [21] reported an extensive study on the effect of different parameters on the topography of gold films deposited on mica. In their study on the effect of temperature, they reported that at room temperature (298 K), a typical topography of a gold film was that of a 'rolling hill'. At 713 K, depending on the film thickness, the topography consisted of long channels. Hence, it was aimed to compare the topography of films produced by clusters in the lower chamber at room temperature and 713 K, where the topography would be expected to be significantly different [21, 22].

Figure 5 shows typical topographies of thin films deposited in the lower chamber at room temperature and 713 ± 20 K (Fig. 5(b)). At 298 K, the film indeed has a rolling hill morphology similar to that produced in other studies. At 713 K the topography had changed to a hilly topography with long channels (Fig. 5(c)), which is also in agreement with Liu *et al.* [21]. Both TEM and AFM results showed that none of the films were porous suggesting that the majority of clusters were charged. Neutral clusters undergo Brownian coagulation, which would result in a porous skeletal fractal-like structure. Hwang *et al.* [1] suggested that the landing behaviors of charged and neutral clusters would be similar to the deflocculation and flocculation of colloid particles, respectively. Overall it can be seen that charged gold clusters produce the thin films presented in this report.

Conclusions

Gold deposition by thermal evaporation was studied in a two-chambered CVD system in order to determine if the CCM applies. The presence of nano-meter sized gold clusters was confirmed by TEM. The charge on the clusters was found to be positive. These charged clusters appear to be the major flux for film formation. This work has also shown that gold thin films deposited on a mica surface in the lower chamber at room temperature resulted from the epitaxial sticking of 4~10 nm clusters. The topography of these films was similar to those reported previously under similar conditions. These nanometer sized clusters resulted from gas phase nucleation in the upper chamber and were transferred to the lower chamber via a 1-mm orifice to produce the film. The highly uniform size of gold clusters is attributed to the presence of charge and might be applied to quantum dot fabrication. Thin film growth by charged clusters appears to be a very general mechanism.

Acknowledgements

This work was supported by the Creative Research Initiative Program of Korea Ministry of Science and Technology.

References

1. N.M. Hwang, J.H. Hahn, and D.Y. Yoon, J. Cryst. Growth 162 (1996) 55.
2. N.M. Hwang, J. Crystal Growth 198/199 (1999) 945.
3. N.M. Hwang, W.S. Cheong, and D.Y. Yoon, J. Crystal Growth 205 (1999) 59.
4. I.D. Jeon, L. Gueroudji, and N.M. Hwang, Korean J. Ceram. 5 (1999) 131.
5. K.S. Seo, Metall. Eng., Chunbuk Univ., Chunju 1998, p. 40.
6. W.S. Cheong, N.M. Hwang, and D.Y. Yoon, J. Crystal Growth 204 (1999) 52.
7. I.D. Jeon, C.J. Park, D.Y. Kim, and N.M. Hwang, In preparation (1999).
8. T. Takagi, Ionized-Cluster Beam Deposition and Epitaxy, Noyes Publications, Park Ridge 1988.
9. H. Fujita, Ultramicroscopy 39 (1991) 369.
10. P. Buffat, J.-P. Borel, Phys. Rev. A 13 (1976) 2287.
11. J.-P. Borel, Surf. Sci. 106 (1981) 1.
12. M. Adachi, K. Okuyama, N. Tohge et al., Jpn. J. Appl. Phys. 31 10A (1992) L1439-L1442.
13. M. Adachi, K. Okuyama, N. Tohge et al., Jpn. J. Appl. Phys. 33 3B (1994) L447-L450.
14. M. Adachi, K. Okuyama, and N. Tohge, J. Mater. Sci. 30 (1995) 932-937.
15. M. Adachi, K. Okuyama, T. Fujimoto et al., Jpn. J. Appl. Phys. 35 8 (1996) 4438-4443.
16. K. Okuyama, T. Fujimoto, and T. Hayashi, AIChE Journal 43 11A (1997) 2688-2697.
17. N.P. Rao, S. Nijhawan, T. Kim et al., J. Electrochem. Soc., 145 6 (1998) 2051-2057.
18. W. Mahoney, S.T. Lin, and R.P. Andres, Mat. Res. Soc. Symp. Proc. 355 (1995) 83.
19. D.R. Lide, CRC Handbook of Chemistry and Physics, 71th ed. 1990-1991.
20. M. Schmidt, R. Kusche, B. von Issendorff, and H. Haberland, Nature 193 (1998) 238.
21. Z.H. Lui and N.M.D. Norman, Thin Solid Films, 300 (1997) 84.
22. M. Levin, A. Laakso, H.E.M. Niemi and P. Hautojarvi, Applied Surface Science, 115 (1997) 31.